

Thin film nanocomposites based on SBM triblock copolymer and silver nanoparticles: morphological and dielectric analysis

Irati Barandiaran¹, Junkal Gutierrez^{1,2}, Agnieszka Tercjak¹, Galder Kortaberria^{1*}

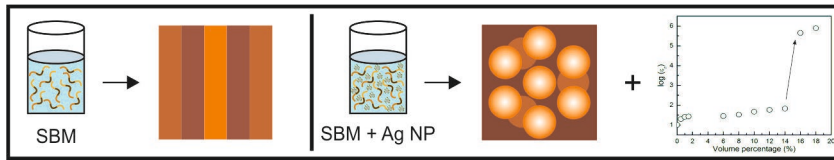
¹I. Barandiaran, J. Gutierrez A. Tercjak, G. Kortaberria.
"Materials + Technologies" Group, Faculty of Engineering, Gipuzkoa, University of the Basque Country UPV/EHU, Plaza Europa 1, 20018 Donostia, Spain

E-mail: galder.cortaberria@ehu.eus

J. Gutierrez

²Faculty of Engineering Vitoria-Gasteiz University of the Basque Country UPV/EHU, C/Nieves Cano 12, 01006 Vitoria-Gasteiz, Spain

Hybrid organic/inorganic thin film nanocomposites based on poly(styrene)-*b*-poly(butadiene)-*b*-poly(methyl methacrylate) (SBM) triblock copolymer and silver nanoparticles (Ag) have been prepared and characterized. In order to improve the compatibility of nanoparticles with the polymeric matrix, their surface has been modified with dodecanethiol surfactant, which enabled a good dispersion of nanoparticles through the triblock copolymer, without the formation of aggregates. By atomic force microscopy (AFM), the dispersion level of nanoparticles has been analyzed, together with their effect on the thin film morphology, for nanocomposites up to 15 wt% of nanoparticles. Dielectric properties of nanocomposites have been studied by dielectric relaxation spectroscopy (DRS), analyzing the effect of nanoparticles on dielectric properties. Even if conductivity and permittivity of composites increased with nanoparticle content, percolation threshold was found to be at around 15 % in volume. Morphologically analyzed nanocomposites were, in this way, below the threshold.



1. Introduction

In recent years the use of nanocomposites based on block copolymers and nanoparticles has attracted attention of many researchers, as they are good candidates for the preparation of new materials with potential advantageous electric or optical properties.^[1-3] Block copolymers are versatile platform materials because they can create a wide variety of nanostructures. They consist in two or more polymer chains (which are thermodynamically incompatible) linked by covalent bonds. Due to this fact, block copolymers can self-assemble into different nanostructures. The morphologies that could be formed because of the self-assembly of block copolymers are various, such as: lamellar, hexagonally packed cylinders, body-centered cubic spheres, double gyroid and perforated layers, among others, depending on several parameters such as molecular weight, volumetric fraction of each block, interactions among blocks and other parameters like annealing process if any, employed solvent, etc.^[4-6] Nowadays many different block copolymers can be found depending on the number of blocks and architecture. Regarding the number of blocks, diblock and triblock copolymers (ABA or ABC type) have been the most used ones. ABC block copolymers are more versatile than diblock or ABA ones, as they can assemble into a higher variety of nanostructures.^[7-9]

Regarding the inorganic component of hybrid materials based on block copolymers, different nanoparticles could be used. Their election mainly depends on the properties that they can provide to the hybrid material. In this direction Song et al.^[10] synthesized Au nanoparticles with optical and electric properties to disperse them into block copolymers, obtaining nanocomposites with high nanoparticle content. Xu et al.^[11] used lead telluride (PbTe) nanoparticles to prepare semiconducting organic/inorganic hybrids based on amphiphilic star-like poly(acrylic acid)-*b*-poly(3,4-ethylene dioxythiophene) (PAA-*b*-PEDOT) diblock copolymers as template. Gutierrez et al.^[12] synthesized TiO₂ nanoparticles by sol-gel technique and dispersed them into polystyrene-*b*-poly(methyl methacrylate) (PS-*b*-PMMA) diblock

copolymers. Magnetic nanoparticles have been also used for preparing copolymer-based nanocomposites. In our previous works, nanocomposites based on different copolymers and magnetic Fe₂O₃ nanoparticles, surface-modified with polymeric brushes, were prepared obtaining a good dispersion of the nanofiller which transmitted magnetic properties to the hybrid materials.^[2, 13, 14]

Among metallic nanoparticles, silver nanoparticles have attracted special attention due to its conductive, optical, antibacterial or catalytic properties. Vural et al.^[15] produced stretchable elastic conductive fibers based on polystyrene-*b*-polyisoprene-*b*-polystyrene (SIS) block copolymer and silver nanoparticles. Moor et al.^[16] combined Ag nanoparticles with C₇₀ to obtain virucidal and bactericidal nanocomposite thin films. In this work they synthesized Ag nanoparticles *in situ* in P4VP nanodomains of poly(styrene)-*b*-poly(4-vinyl pyridine) (PS-*b*-P4VP) diblock copolymers, obtaining selective placement of Ag nanoparticles into P4VP nanodomains and C₇₀ into PS ones. Also Zhao et al.^[17] dispersed Ag nanoparticles into block copolymers. Those researchers obtained hybrid films based on poly(styrene)-*b*-poly(2-vinyl pyridine) (PS-*b*-P2VP) with potential applications in surface enhanced Raman scattering (SERS) and catalyst by Ag nanoparticle addition. Those recent works show the current interest on the research about nanocomposites based on mainly diblock copolymers and Ag nanoparticles, while nanocomposites based on triblock copolymers and nanoparticles have not been so deeply studied.^[13, 18, 19] Within this scenario, in this work organic/inorganic nanocomposites have been prepared based on poly(styrene)-*b*-poly(butadiene)-*b*-poly(methyl methacrylate) (SBM) triblock copolymer and surface-modified Ag nanoparticles. Morphologies of neat copolymer and nanocomposites with Ag nanoparticles have been studied with atomic force microscopy, while dielectric properties have been characterized by dielectric relaxation spectroscopy.

2. Experimental Section

2.1. Materials

SBM triblock copolymer was used as matrix, with a number average molecular weight M_n of 96.142 g/mol, kindly supplied by Arkema, with the following volumetric composition: $f_{PS}=0.3$, $f_{PB}=0.4$ and $f_{PMA}=0.3$. Silver P203 nanoparticles were supplied by Cima Nano Tech, with a specific surface area of 4.9 m²/g and size between 20 and 70 nm. Toluene and dodecanethiol supplied by Sigma Aldrich have been used as solvent and surfactant, respectively.

2.2. Nanocomposite preparation

Toluene was used as solvent for preparing nanocomposite films, as it was found to be an adequate solvent for the copolymer, leading to a surface perpendicular lamellar morphology.^[13] In order to properly disperse nanoparticles, following the procedure used by Peponi et al.,^[20] they were surface-modified with dodecanethiol surfactant. They corroborated that the adequate surfactant/Ag nanoparticle weight ratio should be 1. After sonicating Ag nanoparticles for 1 h, dodecanethiol surfactant was added, and the mixture was further sonicated for 2 h. Sonication was necessary due to the very high surface energy of Ag nanoparticles.^[21] Once nanoparticles were well dispersed with dodecanethiol in toluene, the SBM copolymer was added to the solution. Those solutions were prepared by varying nanoparticle concentration and maintaining block copolymer concentration constant at 5 wt%. Nanocomposite thin films, with a thickness of around 300 nm as measured by AFM, were prepared by casting the solutions onto glass substrates. Nanocomposites with nanoparticle amount varying from 0.5 to 15 wt% were prepared for morphological analysis, while for dielectric measurements and percolation

threshold elucidation nanocomposites with Ag volume content up to 18 % were prepared in order to elucidate the percolation threshold.

2.3. Characterization technique

In this work the morphology and dielectric properties of nanocomposites were characterized. On the one hand, surface morphologies of films with different nanoparticle concentration were studied by AFM with a scanning probe microscopy AFM Dimension ICON of Bruker, operating in tapping mode (TM-AFM). An integrated silicon tip/cantilever, from the same manufacturer, having a resonance frequency of around 300 kHz, was used. Measurements were performed at a scan rate of 1 Hz/s, with 512 scan lines. Thin film surface morphologies were analyzed after 6, 24, 48 h and after 1 month. Taken into account that morphologies of nanocomposite did not change after that time, the morphology obtained after 24 h is presented in this work for each of them. On the other hand, dielectric measurements were carried out with a Dielectric Relaxation Spectroscopy (DRS Novocontrol Alpha high resolution analyzer), working between 1 Hz and 1MHz frequencies, at room temperature. Film samples were placed between two gold plated electrodes in a sandwich configuration.

3. Results and Discussion

Surface morphology of both neat block copolymer and nanocomposite thin films was analyzed by AFM. In our previous work^[13] it was seen that SBM copolymer with that composition ($f_{PS}=0.3$, $f_{PB}=0.4$ and $f_{PMMA}=0.3$) self-assembled into a lamellar nanostructure, as it was predicted by Stadler et al.^[22] for the case of symmetric SBM copolymer, in which the fraction of the middle block was high enough. In **Figure 1** AFM phase and height images of neat SBM block copolymer film can be seen.

The three phases of the block copolymer can be identified. The brightest domain corresponds to PMMA block, the darkest one to PB block and the middle domain to PS one.^[13] Consequently, it can be concluded that SBM triblock copolymer assembled into a lamellar morphology with S-B-M-B sequence and an average interlamellar distance of ~71 nm. The next step was to check if nanoparticles were properly dispersed and if their addition produced morphological changes. **Figure 2** shows AFM phase and height images of nanocomposites with Ag nanoparticles from 0.5 to 5 wt%.

Those figures show that dispersion of nanoparticles through the block copolymer was adequate, as any remarkable nanoparticle aggregate can be detected. By analyzing images in detail, the morphology changes induced by the nanoparticles can be appreciated even at low concentration. For nanocomposite with 0.5 wt% of nanoparticles (Figure 2A) despite lamellar morphology was maintained, some domains started to change, indicating that some cylinders were formed perpendicularly to the surface, as it is indicated by circles in Figure 2A. At higher nanoparticle concentration morphology continued changing, lead to a worm-like morphology for the nanocomposite with 2 wt% (Figure 2B). At 5 wt% of nanoparticles, both in parallel and perpendicularly oriented cylinders can be easily distinguished in AFM images. In order to follow the evolution of morphology with nanoparticle content, AFM images of nanocomposites with higher nanoparticle amount can be observed in **Figure 3**.

As it can be seen, thin film surface morphology of nanocomposites changed completely to spherical one for nanoparticle amount of 15 wt%. In this case, morphology evolved to a spherical one, in which PS and PMMA spheres can be detected in a PB matrix. As for the nanocomposite with 10 wt% some cylinders can still be observed, it could be concluded that the transformation from cylinders to spheres was promoted by nanoparticle addition. In summary, morphology evolved from lamellar to cylinders and from cylinders to spheres with the increase of nanoparticle content, through some intermediate morphologies as wormlike or mixture of both cylinders and spheres. The placement of nanoparticles at copolymer domains

promoted this morphological evolution. Nanoparticle addition could affect system thermodynamics and interaction forces between blocks, modifying the nanostructure as it has been found by other authors.^[14, 23, 24] ABC-type block copolymers have been found to be especially sensitive to nanostructural changes produced by the modification of interactions among blocks,^[25-28] generating unexpected nanostructures in some cases. In this way, Lo et al.^[28] concluded that nanoparticle addition weakened the phase segregation between blocks, while Lin et al.^[24] induced the self-assembly of BCP by adding inorganic nanoparticles, due to a strengthening of interaction forces between blocks. Those examples show the complexity of understanding nanostructures based on triblock copolymers and inorganic nanoparticles.

In order to analyze the placement of nanoparticles at block copolymer domains it is important to consider the solubility parameters of the different polymer chains present in the block copolymer, together with that of the surfactant. Solubility parameters of 19.1, 17.5 and 19.9 can be found for PS, PB and PMMA blocks, respectively, according to Van Krevelen,^[29] the surfactant presents a parameter of 19.1.^[20] According to these values it could be expectable that Ag nanoparticles modified with dodecanethiol surfactant would mainly place at PS domains. Similar result has been found by Hu et al.^[30] working with PS-*b*-PMMA copolymer and dodecanethiol-modified Au nanoparticles, that were placed mainly at PS domains. As nanoparticles cannot be seen in the previous images, in order to visualize them, the organic part of nanocomposites was degraded by UV light irradiation, using a XX-15S UV Bench Lamp with a 254 nm wavelength. Obtained results are shown in **Figure 4** for neat copolymer and nanocomposite with 5 wt% of nanoparticles as an example.

It can be observed that the organic part of the nanocomposite was partially degraded after 96 h. In the case of the neat block copolymer film, even if some clues of the initial morphology can be appreciated, the lamellar morphology disappeared. In the images corresponding to the nanocomposite, Ag nanoparticles can be easily distinguished in the partially degraded SBM copolymer (Figures D1 and D2), well dispersed through the block copolymer, without any

remarkable aggregate, even if their location at specific domains cannot be elucidated by AFM images.

Regarding dielectric characterization, **Figure 5** shows the evolution of dielectric permittivity (ϵ_r) and conductivity (σ) with volume percentage of Ag nanoparticles at a frequency of 1 MHz. First four points in the graphs correspond to nanocomposites with nanoparticle weight fractions of 0, 5, 10 and 15 % (0, 0.5, 1 and 1.57 % in volume, respectively), analyzed above by AFM. As it can be observed, there is a slight increase of both relative permittivity and conductivity with Ag content, the sharp increase of several orders of magnitude in dielectric parameters occurring between 14 and 16 % of nanoparticle volume percentage, indicating that percolation threshold is around 15-16 %. This value is close to those found by other authors for composites based on PVDF and Ag nanoparticles with a size lower than 100 nm, similar to those used in this work.^[31] For nanoparticle content below percolation threshold, observed increase can be due to the interfacial Maxwell-Wagner-Sillars polarization,^[31-33] derived from the accumulation of charges at the interfaces between two phases with different permittivity and conductivity values generated by nanoparticle addition. The value of 15-16 % in volume for percolation threshold seemed to indicate that, for lower nanoparticle content as it is the case for the nanocomposites whose morphology has been studied in this work in which Ag content was much lower than the percolation threshold (i.e. the nanocomposite with 15 wt% of nanoparticles corresponds to a volume fraction of around 1.5 % in volume), nanoparticles were well dispersed through the matrix, without interactions or coupling between them and almost without electron hopping to adjacent nanoparticles,^[31, 34] nanocomposites appearing as non-conductive up to around 15-16 % in volume. From this value, the coupling seemed to occur between nanoparticle domains, promoting electron hopping among them and rendering nanocomposites conductive. Thus, nanocomposites analyzed by AFM in this work were well below the percolation threshold, with a good distribution of nanoparticles through polymeric matrix.

4. Conclusions

The main conclusions obtained from this work are the following. SBM triblock copolymer could be an adequate candidate to prepare hybrid organic/inorganic nanocomposites, as it gives the opportunity to host high quantities of surface-modified nanoparticles without forming big aggregates at least for nanoparticle amount up to 15 wt%, showing also that dodecanethiol could be a good surfactant to disperse Ag nanoparticles. This nanoparticle addition seemed to affect the interactions between blocks, inducing a morphological change at the surface from lamellar to cylinders and from cylinders to spheres with the increase of nanoparticle content, through some intermediate morphologies as wormlike one or mixture of cylinders and spheres.

From dielectric measurements it has been probed that nanocomposites were well below the percolation threshold, even if the conductivity and permittivity of nanocomposites increased with nanoparticle content mainly due to interfacial polarization. A percolation threshold of around 15-16% in volume has been found, similar to that found by other authors for composites based on polymeric matrix and Ag nanoparticles of similar size.

Acknowledgements: Financial support from the Basque Country Government (Grupos Consolidados, IT776-13) and the Spanish Ministry of Economy And Competitiveness and European Community in the frame of MAT2015-66149-P project is gratefully acknowledged.

Received: Month XX, XXXX; Revised: Month XX, XXXX; Published online:

((For PPP, use “Accepted: Month XX, XXXX” instead of “Published online”)); DOI: 10.1002/marc.((insert number)) ((or ppap., mabi., macp., mame., mren., mats.))

Keywords: Block copolymer, thin film nanocomposite, Ag nanoparticle, AFM, DRS

- [1] S. Sanwaria S. Singh, A. Horechyy, P. Formanek, M. Stamm, R. Srivastavaa, B. Nandan, *RSC Adv.* **2015**, 5, 89861.
- [2] I. Barandiaran, G. Kortaberria, *RSC Adv.* **2015**, 5, 95840.
- [3] H. Etxeberria, A. Tercjak, I. Mondragon, A. Eceiza, G. Kortaberria, *Colloid Polym. Sci.* **2014**, 292, 229.
- [4] N. Politakos, E. Ntoukas, A. Avgeropoulos, V. Krikorian, B. D. Pate, E. L. Thomas, R. M. Hill, *J. Polym. Sci. Pt. B-Polym. Phys.* **2009**, 47, 2419.
- [5] I. Zalakain, J. A. Ramos, R. Fernandez, H. Etxeberria, I. Mondragon, *Thin Solid Films* **2009**, 519, 1882.
- [6] I. Zalakain, J. A. Ramos, R. Fernandez, H. Etxeberria, I. Mondragon, *J. Appl. Polym. Sci.* **2012**, 125, 1552.
- [7] T. I. Löbbling, P. Hiekkataipale, A. Hanisch, F. Bennet, H. Schmalz, O. Ikkala O, A. H. Gröschel, A. H. E. Müller, *Polymer* **2015**, 72, 479.
- [8] H. Hückstädt, A. Göpfert, V. Abetz, *Polymer* **2000**, 41, 9089.
- [9] K. Fukunaga, T. Hashimoto, H. Elbs, G. Krausch, *Macromolecules* **2003**, 36, 2852.
- [10] D. P. Song, Y. Lin, Y. Gai, N. S. Colella, C. Li, X. H. Liu, S. Gido, J. J. Watkins, *J. Am. Chem. Soc.* **2015**, 137, 3771.
- [11] H. Xu, X. Pang, Y. He, M. He, J. Jung, H. Xia, Z. Lin, *Angew. Chem.-Int. Edit.* **2015**, 54, 4636.
- [12] J. Gutierrez, A. Tercjak, I. Garcia, I. Mondragon, *Nanotechnology* **2009**, 20, 225603.
- [13] I. Barandiaran, G. Kortaberria, *Eur. Polym. J.* **2016**, 78, 340.
- [14] I. Barandiaran, E. Grana, D. Katsigiannopoulos, A. Avgeropoulos, G. Kortaberria, *Eur. Polym. J.* **2016**, 75, 514.
- [15] M. Vural, A. M. Behrens, O. B. Ayyub, J. J. Ayoub, P. Kofinas, *ACS Nano* **2015**, 9, 336.

- [16] K. J. Moor, C. O. Osuji, J. H. Kim, *ACS Appl. Mater. Interfaces* **2016**, 8, 33583.
- [17] X. Zhao, Q. Wang, X. Yu, Y. Lee, H. G. Liu, *Colloid Surf. A-Physicochem. Eng. Asp.* **2017**, 516, 171.
- [18] T. Périé, A. C. Brosse, S. Tencé-Girault, L. Leibler, *Polymer* **2011**, 52, 3065.
- [19] T. Périé, A. C. Brosse, S. Tencé-Girault, L. Leibler, *Carbon* **2012**, 50, 2918.
- [20] L. Peponi, A. Tercjak, L. Torre, J. M. Kenny, I. Mondragon *Compos. Sci. Technol.* **2008**, 68, 1631.
- [21] W. Caseri, *Macromol Rapid Commun*, **2000**, 21, 705.
- [22] R. Stadler, C. Auschra, J. Beckmann, U. Krappe, I. Voigt-Martin, L. Leibler, *Macromolecules* **1995**, 28, 3080.
- [23] S.-W. Yeh, K.-H. Wei, Y.-S. Sun, U-S. Jeng, K.S. Liang, *Macromolecules* **2005**, 38, 6559.
- [24] Y. Lin, V. K. Daga, E. R. Anderson, S. P. Gido, J. J. Watkins, *J. Am. Chem. Soc.* **2011**, 133, 6513.
- [25] T. I. Löbbling, P. Hiekkataipale, A. Hanisch, F. Bennet, H. Schmalz, O. Ikkala, A. H. Gröschel, A. H. E. Müller, *Polymer* **2015**, 72, 479.
- [26] U. Nagpal, F. A. Detcheverry, P. F. Nealy, J. J. de Pablo, *Macromolecules* **2011**, 44, 5490.
- [27] C. Tang, J. Bang, G. E. Stein, G. H. Fredrickson, C. J. Hawker, E. J. Kramer, M. Sprung, J. Wang, *Macromolecules* **2008**, 41, 4328.
- [28] C. T. Lo, B. Lee, V.G. Pol, N.L. Dietz Rago, S. Seifert, R.E. Winans, P. Thiyagarajan, *Macromolecules* **2007**, 40, 8302.
- [29] D. W. Van Krevelen, *Properties of polymers*, Elsevier, Amsterdam, Elsevier Scientific Publishing Co. **1990**
- [30] S. Hu, W. J. Brittain, S. Jacobson, A. C. Balazs, *Eur. Polym. J.* **2016**, 42, 2045.
- [31] K. S. Deepa, M. S. Gopika, J. James, *Compos. Sci. Technol.* **2013**, 78, 18.

[32] V. Singh, A. R. Kulkarni, T. R. Rama Mohan. *J. Appl. Polym. Sci.* **2003**, 90, 3602.

[33] G. Kortaberria, P. Arruti, I. Mondragon, *Polym. Int.* **2001**, 50, 957.

[34] K. S. Deepa, M. T. Sebastian, J. James, *Appl. Phys. Lett.* **2007**, 91, 202904.

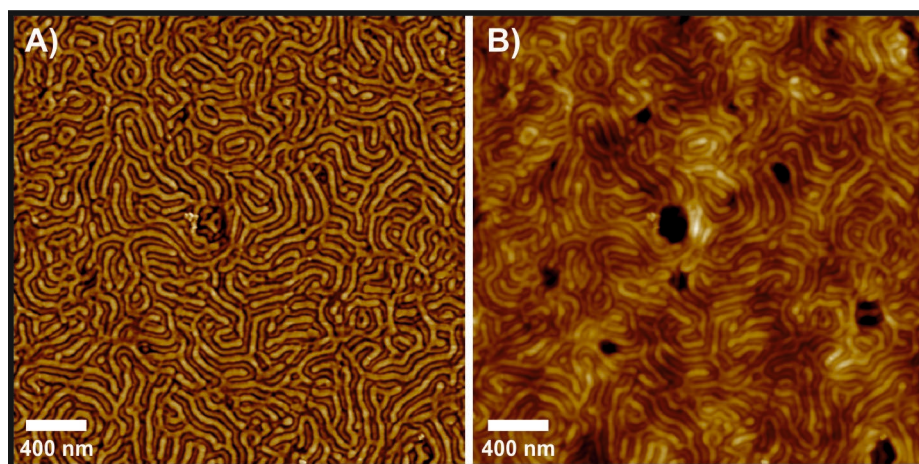


Figure 1. AFM phase (A) and height (B) images of neat SBM triblock copolymer thin film.

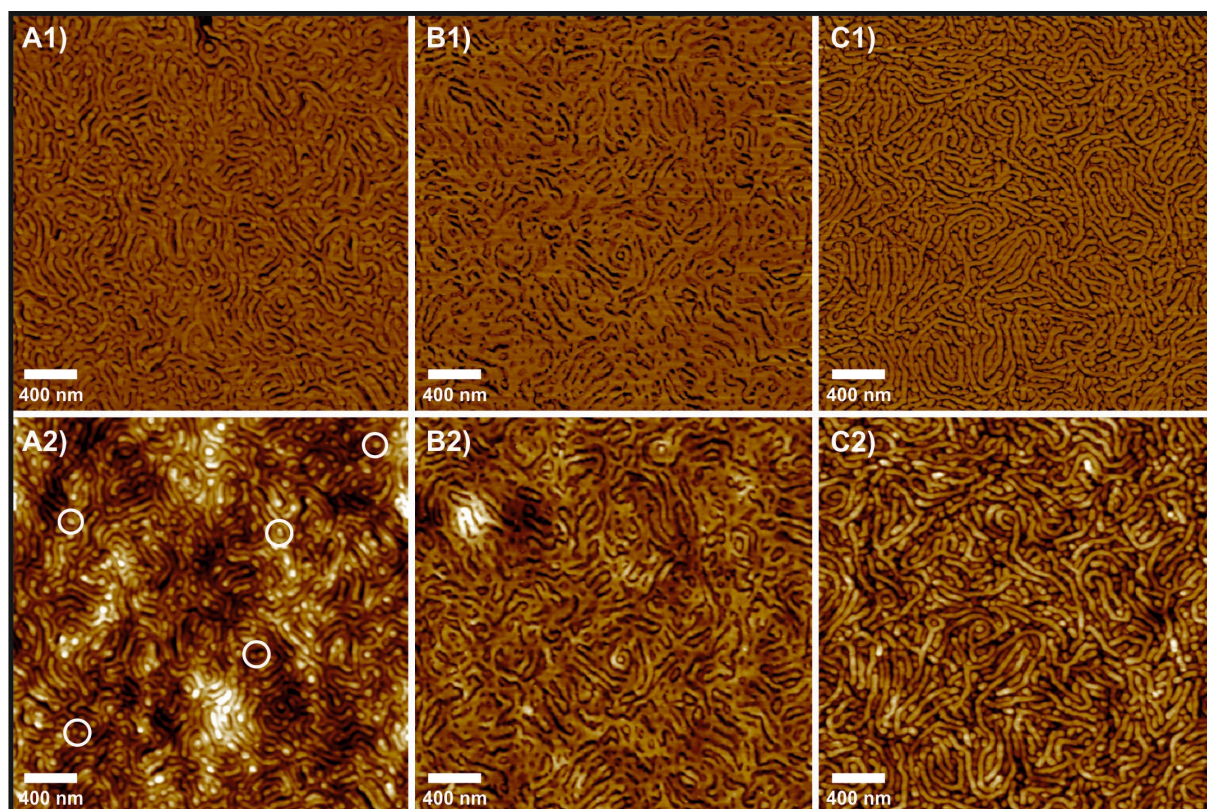


Figure 2. AFM phase (1) and height (2) images of nanocomposite thin films with (A) 0.5, (B) 2 and (C) 5 wt% of nanoparticles.

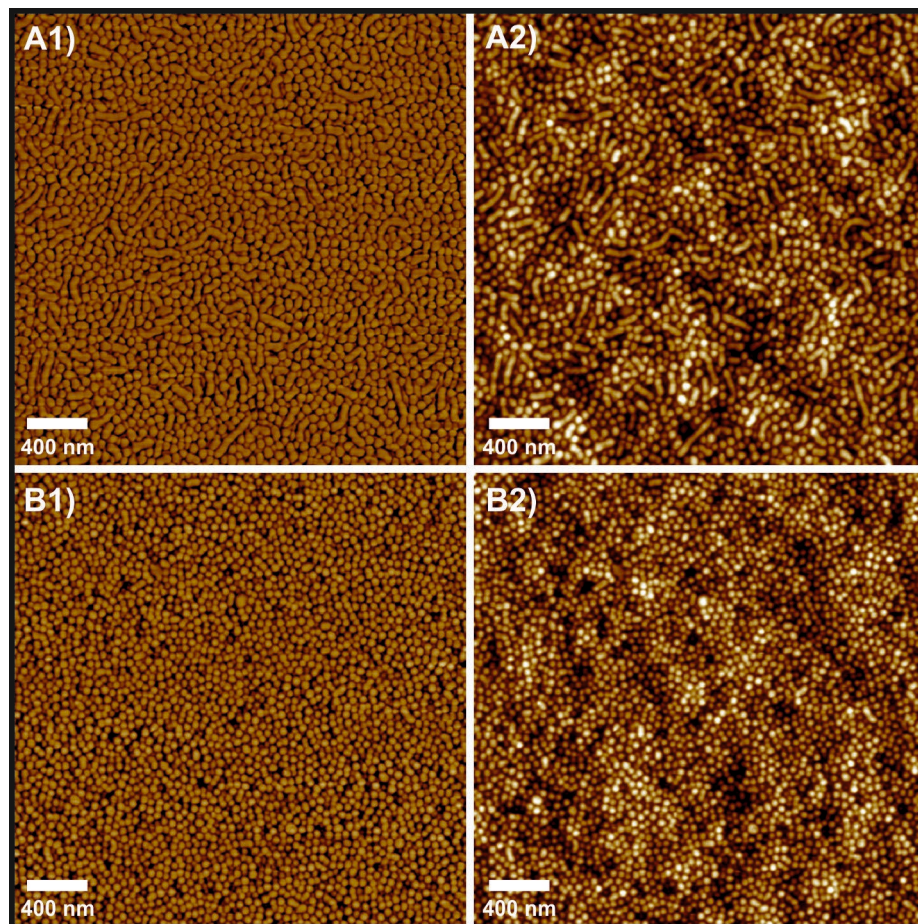


Figure 3. AFM phase (1) and height (2) images of nanocomposites with (A) 10 and (B) 15 wt% of nanoparticles.

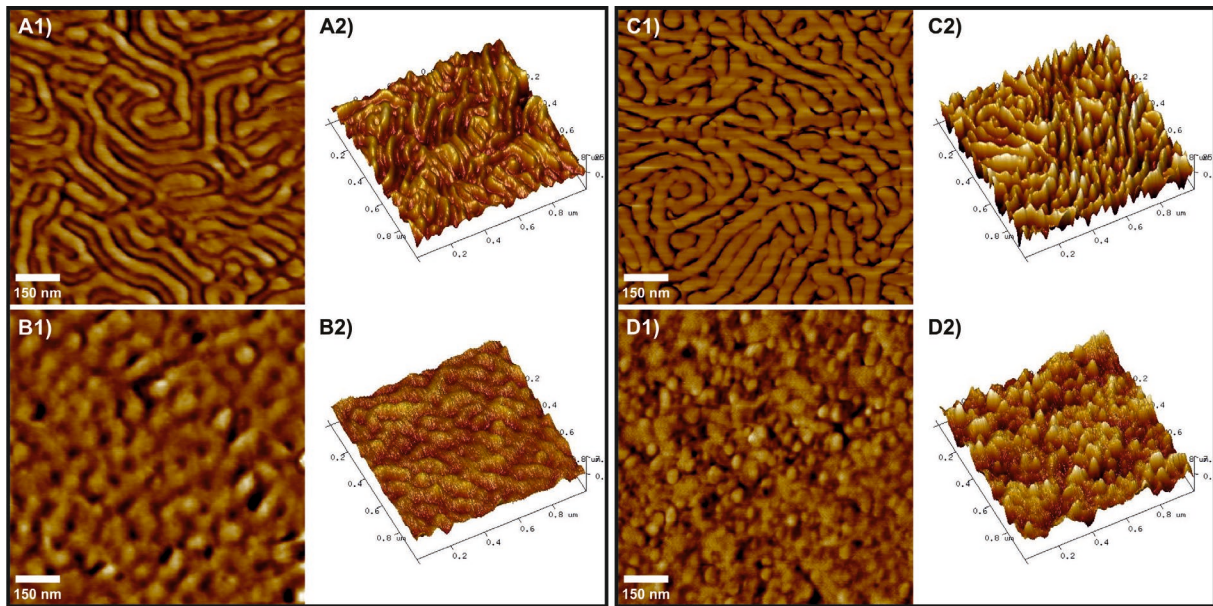


Figure 4. AFM phase (1) and 3D height (2) images of neat block copolymer before (A) and after (B) UV light treatment for 96 h and of nanocomposite with 5 wt% of nanoparticles (C) before and (D) after UV light treatment for 96 h.

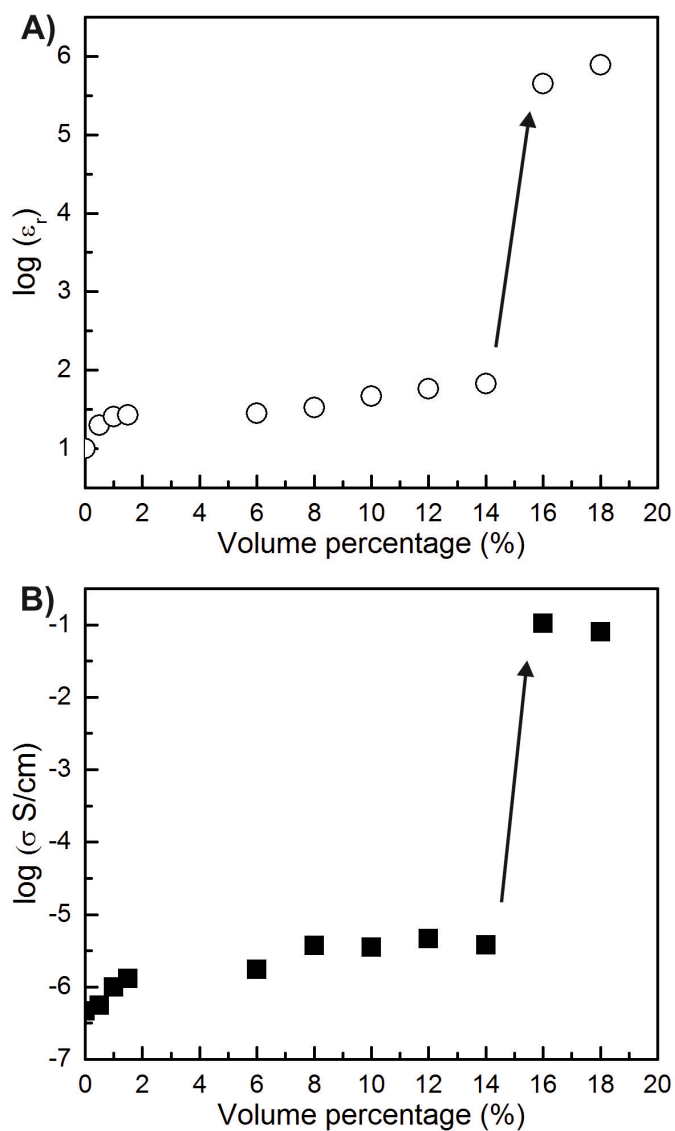


Figure 5. Evolution of (A) relative permittivity and (B) conductivity compared to nanoparticle volume fraction.

I. Barandiaran, J. Gutierrez, A. Tercjak, G. Kortaberria*

Thin film nanocomposites based on SBM triblock copolymer and silver nanoparticles: morphological and dielectric analysis

